

Microgrid Integration Based on Deep Learning NARMA-L2 Controller for Maximum Power Point Tracking

Enas Hamid Ibrahim^{1,*}, Nadia Qasim Mohamed², Hanan Mikhael D.Habbi³

^{1,2,3} Department of Electricity Engineering, College of Engineering, University of Baghdad, Baghdad, Iraq

³ Electrical and Computer Engineering, Oakland University, Michigan, USA

enas.hamid@coeng.uobaghdad.edu.iq¹, nadia.qasim@coeng.uobaghdad.edu.iq², hhabbi@oakland.edu³

ABSTRACT

This paper presents a hybrid energy resources (HER) system consisting of solar PV, storage, and utility grid. It is a challenge in real time to extract maximum power point (MPP) from the PV solar under variations of the irradiance strength. This work addresses challenges in identifying global MPP, dynamic algorithm behavior, tracking speed, adaptability to changing conditions, and accuracy. Shallow Neural Networks using the deep learning NARMA-L2 controller have been proposed. It is modeled to predict the reference voltage under different irradiance. The dynamic PV solar and nonlinearity have been trained to track the maximum power drawn from the PV solar systems in real time.

Moreover, the proposed controller is tested under static and dynamic load conditions. The simulation and models are done by using MATLAB/Simulink. The simulation results from the proposed NARMA-L2 controller have been compared with existing Perturb and observe PO-MPPT and Incremental Conductance INC -MPPT methods.

Keywords: Microgrid, Solar PV, HER, Maximum power point tracking, Deep learning, PO-MPPT, INC-MPPT.

*Corresponding author

Peer review under the responsibility of University of Baghdad.

<https://doi.org/10.31026/j.eng.2023.10.02>

This is an open access article under the CC BY 4 license (<http://creativecommons.org/licenses/by/4.0/>).

Article received: 07/04/2023

Article accepted: 04/06/2023

Article published: 01/10/2023



الشبكة الصغيرة المتكاملة باستخدام تحكم التعلم العميق NARMA-L2 لأقصى تتبع لنقطة الطاقة

ايناس حامد ابراهيم¹،*، نادية قاسم محمد²، حنان ميخائيل داود حبي³

قسم الهندسة الكهربائية، كلية الهندسة، جامعة بغداد، بغداد، العراق
هندسة الكهرباء والحاسبات، جامعة اوكلاند، مشيغان، لولايات المتحدة الامريكية

الخلاصة

يقدم هذا البحث نظام موارد الطاقة الهجين (HER) الذي يتكون من أنظمة الطاقة الشمسية الكهروضوئية، ونظام التخزين، والشبكة الكهربائية. يوفر النظام الأحمال الثابتة والأحمال الديناميكية تعتبر خوارزميات حساب أعظم قدرة لأنظمة الخلايا الشمسية خلال الزمن الحقيقي من التحديات وخصوصا عندما تكون شدة الاشعاع الشمسي متغيرة. وتتخلص بعض التحديات في إيجاد نقطة أعظم قدرة واداء الخوارزمية الديناميكي وأيضا سرعة الحصول على مقدار أعظم قدرة وكذلك الدقة والتكيف مع المتغيرات. تم اقتراح في هذا البحث استخدام الشبكات العصبية الضحلة باستخدام وحدة التحكم NARMA-L2 التي صممت من خلال تحديد الفولتية المرجعية اثناء تغيير شدة الاشعاع الشمسي تم تدريب النظام الكهروضوئي الديناميكي وغير الخطي لتتبع الطاقة القصوى المستمدة من أنظمة الطاقة الشمسية الكهروضوئية في الوقت الحقيقي. لتعظيم الطاقة الناتجة من الطاقة الشمسية الكهروضوئية يتم الحصول عليها من خلال محول التعزيز وتحت ظروف تحميل مختلفة. تتم المحاكاة والنماذج باستخدام MATLAB / Simulink. تمت مقارنة نتائج المحاكاة من وحدة التحكم NARMA-L2 المقترحة مع طرق PO-MPPT وطرق INC-MPPT.

الكلمات المفتاحية: الشبكة الصغيرة، الطاقة الشمسية الكهروضوئية، HER، أقصى تتبع نقطة الطاقة، التعلم العميق، - INC، MPPT، PO-MPPT.

1. INTRODUCTION

Renewable energy sources such as solar PV have increased significantly, especially recently (Wen et al., 2019; Singh et al., 2022). However, increasing power penetration on a microgrid may cause problems such as voltage deviation, surges, and frequency fluctuations. Predicting the maximum power drawn from the PV system may enable better voltage and current responses (Abdul Hussain and Habbi, 2018; Kulkarni and Deshmukh, 2019). Therefore, extracting maximum power with good transient performance is a challenge. The exciting MPPT methods have disadvantages with partial shading in PV and solar temperature and load conditions (Chen et al., 2022; Jamil et al., 2022; Singh et al., 2022). MPPT algorithms had many difficulties in partial shading conditions due to obstructions such as buildings, cloudy weather, trees, etc. These difficulties might lead to more points of local maximum power, and consequently, the conventional MPPT algorithms, such as PO and INC, may struggle to identify accurately the global MPP. In verse, in these situations, it could stick in local MPPT. Another matter, partial shading causes rapid oscillations in the output voltage and currents of the solar PV panel. These oscillations may lead to misleading toward the incorrect tracking of MPP. The voltage and current oscillations influence the microgrid efficiency and reduce the lifetime of the power electronic switches. Besides that, the sudden



and dynamic behavior of the MPPT algorithms during shading conditions made the conventional methods respond immediately. As some of the MPPT methods take significantly longer than the global MPP, this will affect reducing the energy extracted during the variation of the irradiance (**Alcaide et al., 2022; Dagal et al., 2022; Isknan et al., 2023; Pervez et al., 2022**).

Some researchers studied the impact of measurement errors caused by shading conditions (**Jane et al., 2022; Millah et al., 2022**). The PV solar and nonuniform configuration design may induce an imbalance in power losses (**Habbi and Alhamadani, 2018**). Therefore, using an effective MPPT under partial shading limits the microgrid performance (**Burlacu and Navrapescu, 2022; Rao and Sundaramoorthy, 2022**).

Maximum power point tracking has been used with the boost converter since the MPPT generates the switching pulses for the dc-to-dc converter (**Zhou et al., 2016**). The DC voltage of the inverter is independent of (**Millah et al., 2021; Gadiraju, 2022**) the output voltage of the solar PV. PO-MPPT had a problem with steady state oscillations near to maximum point and in local tracking instead of globally in partial shading conditions (**Kulkarni and Deshmukh, 2019; Vanti et al., 2022**). On the other hand, the INC-MPPT has higher accuracy than the PO-MPPT, but it is more complex due to its dynamic operation and selecting the step size, which is becoming smaller, reaching the steady-state error (**Paduani et al., 2022**). That will lead to concluding that the conventional MPPT algorithms had the demerits of inaccurate output power setting and oscillation because of the slow tracking of the calculation (**Kulkarni and Deshmukh, 2019; Awan et al., 2022; Yang et al., 2023**).

A recurrent neural network has been used for load demand forecasting in smart grids. This scenario is accomplished based on the consumer demand pattern (**Kaushal and Basak, 2020; Nhung et al., 2022**). Hybrid Fuzzy-particle swarm optimization-based grid system has been used to predict the model to improve the accuracy, but it has limited performance when the data are huge (**Azeem et al., 2022**).

Addressing the challenges mentioned above and problems during the operation of solar PV under partial shading. This paper proposed a NARMA-L2 controller to use and obtain the maximum power in the microgrid-connected system during partial shading. This controller depends on real-time information and tracks the global MPP accurately, even in partial shading conditions. The simulation results are obtained and compared with conventional methods such as Perturb and observe (PO-MPPT) and Incremental Conductance (INC - MPPT) (**Mohamed and Habbi, 2020; Jamil et al., 2022**). Afterward, two loads (static and dynamic) were used to test the proposed controller. In addition, the proposed controller is tested with constant and variable solar irradiances.

This paper aims to control the maximum power point of an integrated microgrid during partial shading conditions (i.e., variable solar irradiance). The proposed controller is Shallow Neural Networks using the deep learning NARMA-L2 controller. The modeling uses the prediction of the reference voltage under different irradiance. However, dynamic PV solar has been trained to track the maximum power drawn from the PV solar systems in real time.

2. THE PROPOSED METHODOLOGY

It's a challenge to extract the controller for obtaining the maximum power from a PV solar with variations of solar irradiance and temperature (**Jamil et al., 2022**). The plant identification process lets training a neural network to model the grid. It should identify the grid before training the controller whenever it is unsatisfied. The controller needs to be

identified (Wen et al., 2019; Saadaoui et al., 2023). The proposed microgrid consists of solar PV, a utility grid, an energy storage system, and a load, as shown in Fig. 1.

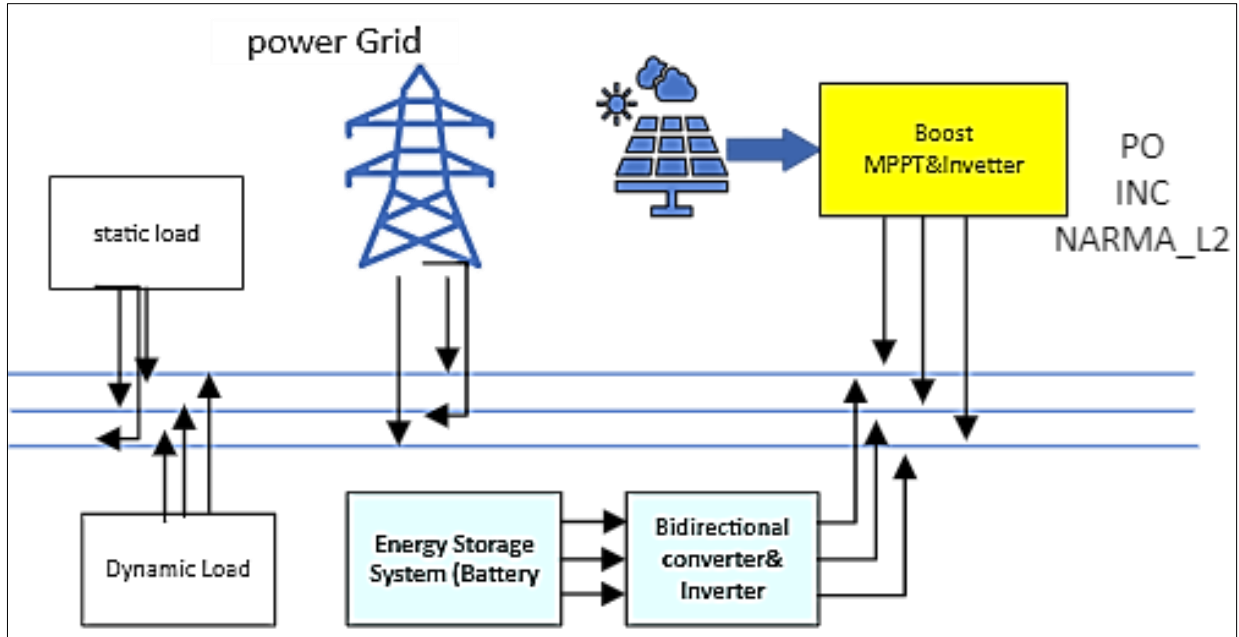


Figure 1. Microgrid system diagram

3. THE SYSTEM MODELING

The system is implemented with MATLAB/Simulink, as shown in Fig. 2.

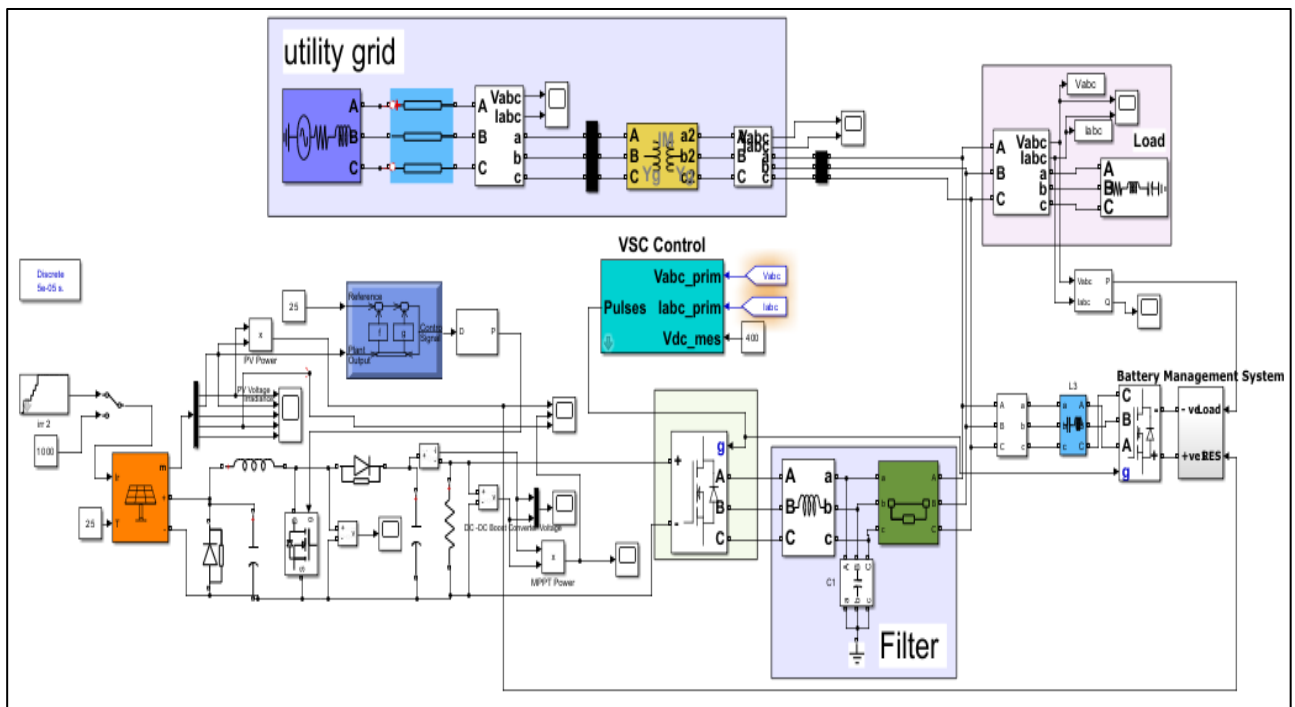


Figure 2. Proposed NARMA-L2 controller with microgrid MATLAB/Simulink

3.1 Load Model

The loads consist of static and dynamic, as given in **Table 1**.

Table 1. Load specifications

Load type	Parameters
RL load	10 kW active power and reactive power of 5 kVar
Induction motor	3-phase,5HP, 400V,50Hz

3.2 PV Solar System Model

The equivalent circuit of the PV cell is shown in **Fig. 3**. The mathematical equations are given as the following equations (**Pendem and Mikkili, 2018; Rao and Sundaramoorthy, 2022**)

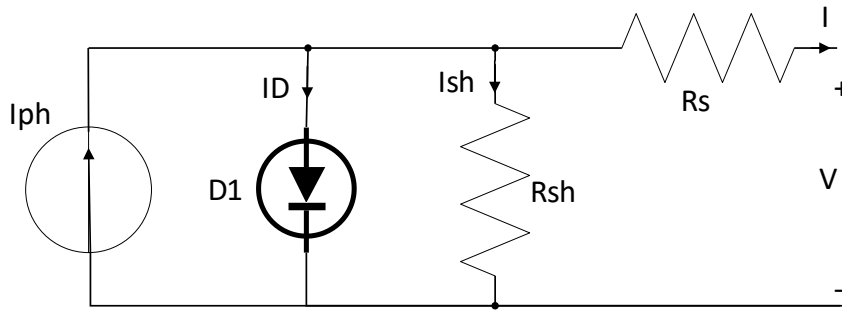


Figure 3. PV cell equivalent circuit (**Chauhan and Singh, 2022**)

$$I_o = I_{sh} / [\exp\left(\frac{qV_T}{N_s k n T}\right) - 1] \tag{1}$$

$$I_{sh} = \frac{V \times \frac{N_p}{N_s} + I R_s}{R_{sh}} \tag{2}$$

The I/V and P/V characteristics are shown in **Fig. 4** under different irradiance and specified temperatures of 25 °C. The solar PV parameters for the simulation are presented as follows: MPP is 10100W at 25Co, a current of 42A, and a voltage of 390V. The DC voltage will decrease when the temperature increases when the irradiance is 1000W/m².

Fig. 5 gives the PV specification. **Fig. 6** shows the block diagram for the solar PV model based on the MPPT boost converter. The two conventional MPPT, P&O and INC -MPPT algorithms, have been used. The codes are given in Appendix A for both methods (**Abdul Hussain and Habbi, 2018; Kulkarni and Deshmukh, 2019; Ahmed et al., 2022**).

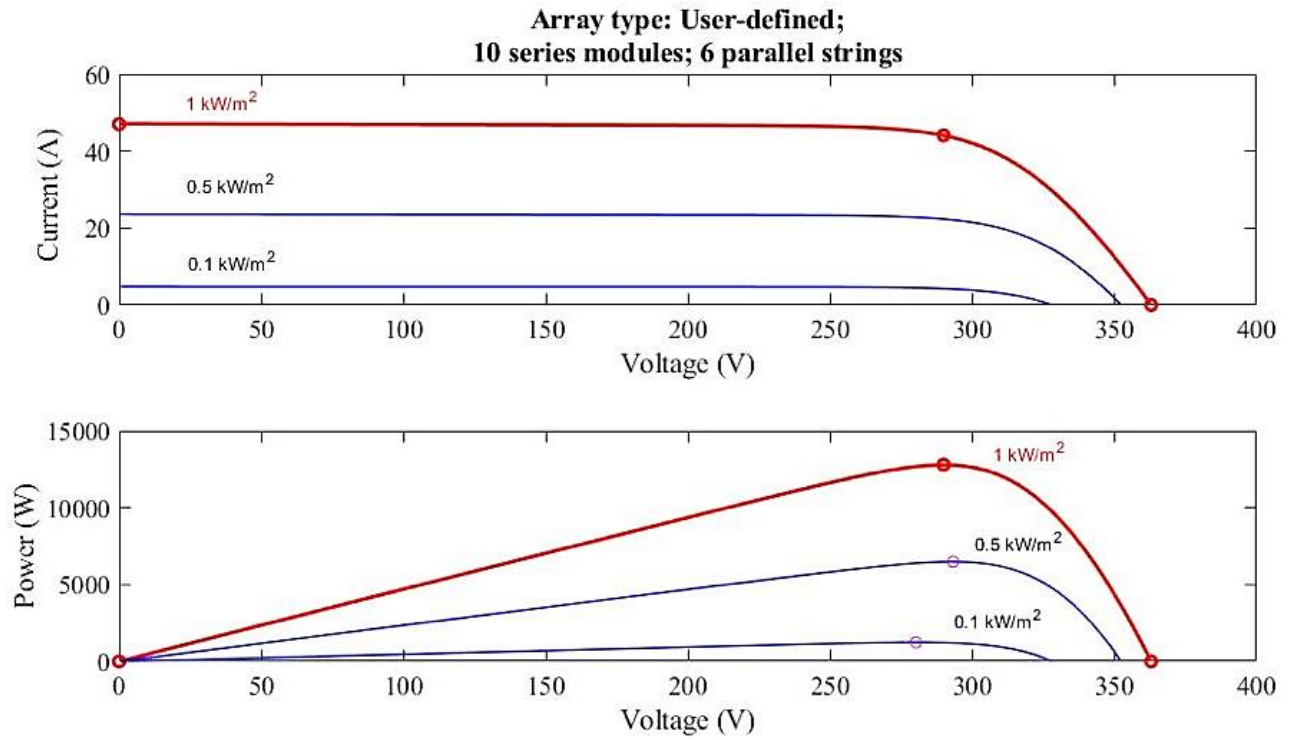


Figure 4. I/V and P/V characteristics of the PV cell

Module data	
Module:	User-defined
Maximum Power (W)	213.15
Cells per module (Ncell)	60
Open circuit voltage Voc (V)	36.3
Short-circuit current Isc (A)	7.84
Voltage at maximum power point Vmp (V)	29
Current at maximum power point Imp (A)	7.35
Temperature coefficient of Voc (%/deg.C)	-0.36099
Temperature coefficient of Isc (%/deg.C)	0.102

Figure 5. MATLAB/Toolbox PV Panel Specification

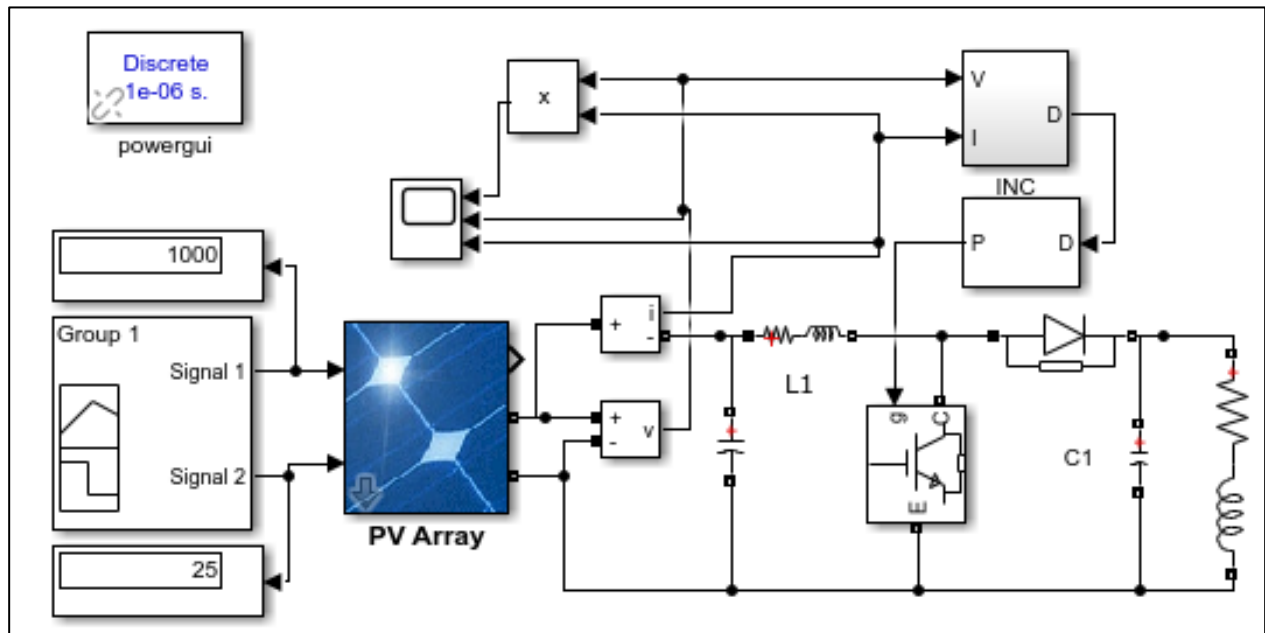


Figure 6. Solar PV with boost converter based on MPPT

The proposed MPPT method is based on a deep learning toolbox NARMA-L2 controller. The required parameters that need to be identified are:

- Hidden layer size requires to use number of neurons in the hidden layer of the neural network grid system.
- Train the neural network grid system.
- Controller outputs are overdue to serve the neural network grid system.
- Sampling time is used to collect data for the training process.
- The identification process requires a training function.
- The identification process started with importing the training data entered from the training grid.
- The training samples generate the training data depending on the limits of input and output data.
- The range of input-output data will be within 0-1.
- Selecting the number of epochs during training.
- A quarter of the training data will be used for testing and validation.

The flow chart for implementing deep learning NARMA-L2 is shown in **Fig. 7**.

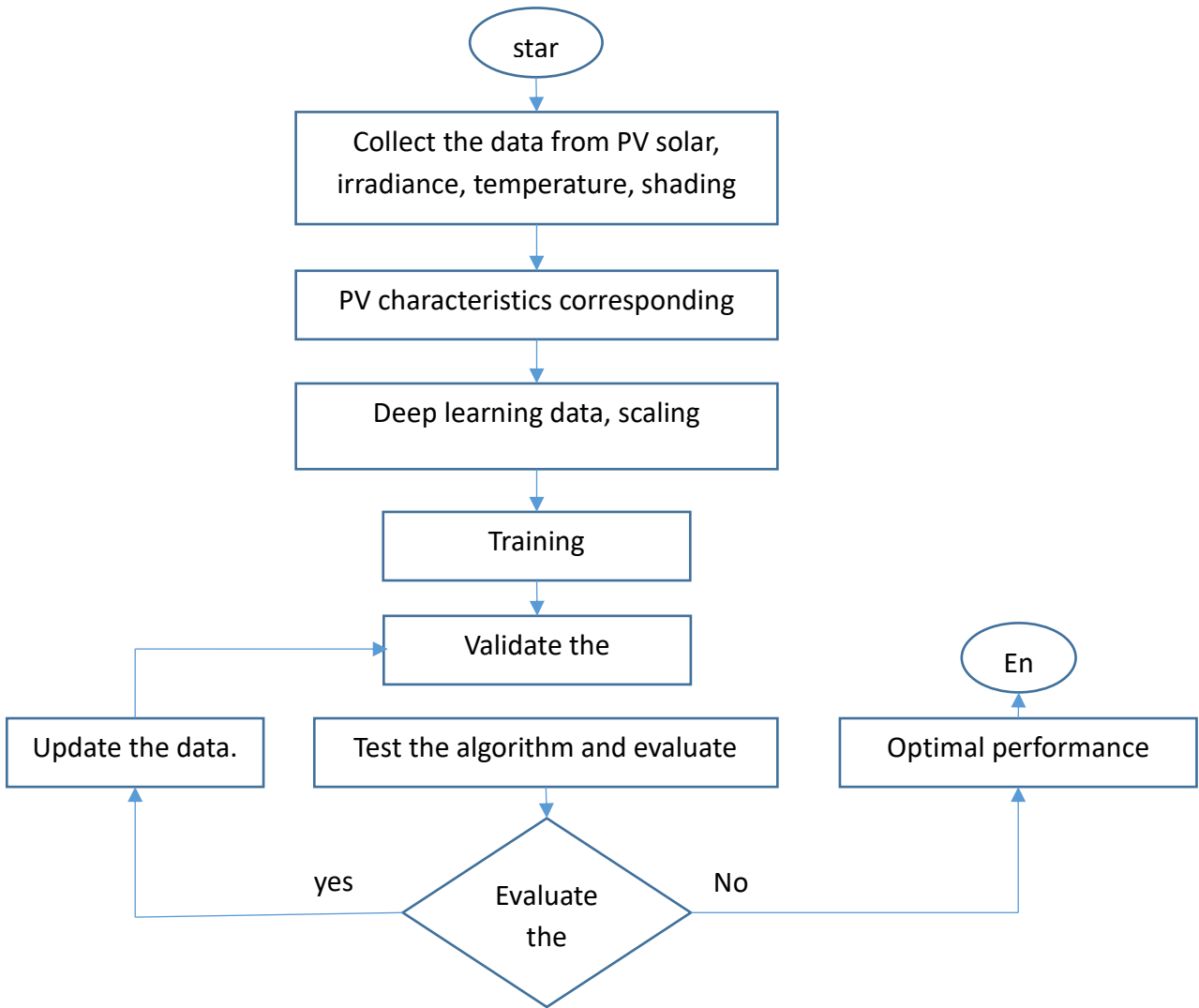


Figure 7. NARAMA-L2 flowchart

The schematic of the NARMA-L2 controller is shown in Fig. 8. The plant identification is shown in Fig. 9.

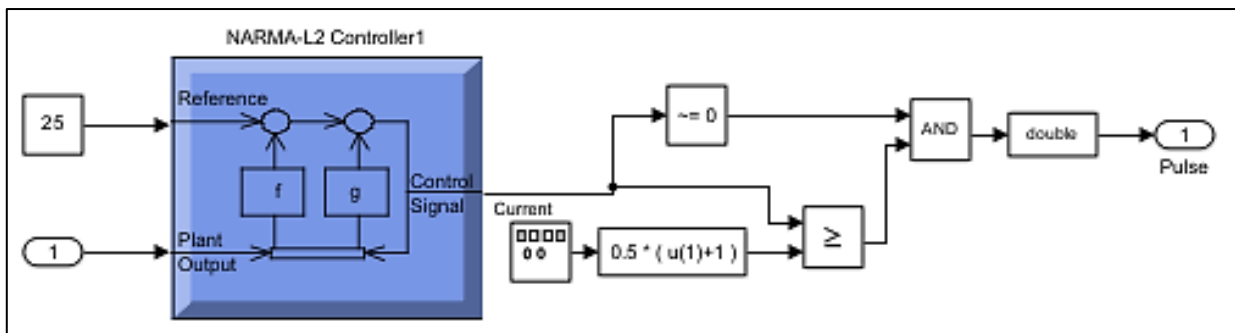


Figure 8. NARAMA-L2 controller scheme

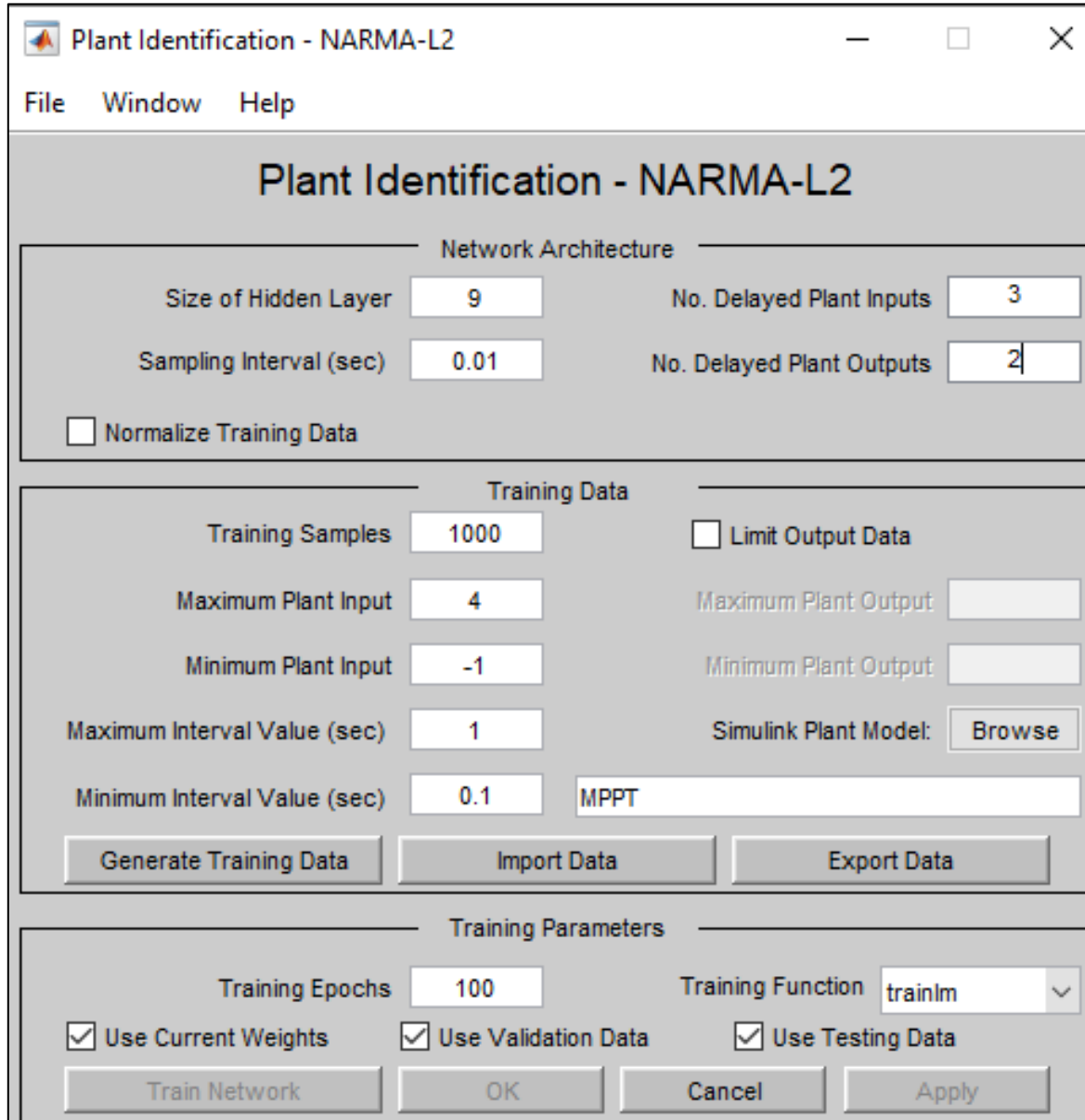


Figure 9. Plant Identification deep learning toolbox NARMA-L2 controller

The identification of the NARMA-L2 controller model is contained in the deep learning toolbox. This controller will change the nonlinear dynamic system into a linear one (**Nhung et al., 2022**). The mathematical identification neural network model is derived as follows:

$$y\{t + d\} = F[y(t), y(t - 1), \dots, y(t - n + 1), u(t), u(t - 1), \dots, u(t - n + 1)] \quad (3)$$

where $u(t)$ is the system input, and $y(t)$ is the system output. The neural network is trained in the nonlinear function F . Then, the system output is

$$y\{t + d\} = ym(t + d) \quad (4)$$

The nonlinear controller is developed as follows:



$$u\{t\} = A[y(t), y(t - 1), \dots, y(t - n + 1), y(t + d), u(t - 1), \dots, u(t - r + 1)] \quad (5)$$

Creating the function (A) was a problem that minimizes the mean square error. The controller model will be:

$$y\{t + d\} = g[y(t), y(t - 1), \dots, y(t - n + 1), \dots, u(t - n + 1)] + f[y(t), y(t - 1), \dots, y(t - n + 1), u(t - 1), \dots, u(t - r + 1)] \cdot u(t) \quad (6)$$

The next controller input, $u(t)$, does not contain the nonlinearity. Then the system output follows the reference $y(t + d) = y_m(t + d)$.

The model results in:

$$u\{t\} = y_m(t + d) - g[y(t), y(t - 1), \dots, y(t - n + 1), \dots, u(t - n + 1)] + f[y(t), y(t - 1), \dots, y(t - n + 1), u(t - 1), \dots, u(t - r + 1)] \quad (7)$$

Determine the control input $u(t)$ based on the output at the same time $y(t)$. Therefore, the following model was used.

$$y(t + d) = g[y(t), y(t - 1), \dots, y(t - n + 1), \dots, u(t - n + 1)] + f[y(t), y(t - 1), \dots, y(t - n + 1), u(t - 1), \dots, u(t - r + 1)] \cdot u(t + 1) \quad (8)$$

3.3 Battery Storage Model

The battery storage system is concerned with the microgrid to compensate for the fluctuations in the renewable energy penetration. This system depends on the microgrid's charging and discharging requirements (Asadi et al., 2023; He et al., 2023).

The constraints of the state of charge equation are given as follows:

$$SOC_{min} < SOC < SOC_{max} \quad (9)$$

The battery's SOC is limited to 30% and 70% of its power in ampere-hour capacity. It prevents the battery life from undercharging or overcharging.

The limits of the charging battery power are

$$P_{battmin} < P_{battcharging} < P_{battmax} \quad (10)$$

The limits of the discharging battery power are

$$P_{battmin} < P_{battdischarging} < P_{battmax} \quad (11)$$

The proposed bidirectional controller for the battery storage is modeled with Matlab/Simulink, as shown in Fig. 10. It is clear that the battery will charge or /discharge depending on the degradation between the power generation and the load demands.

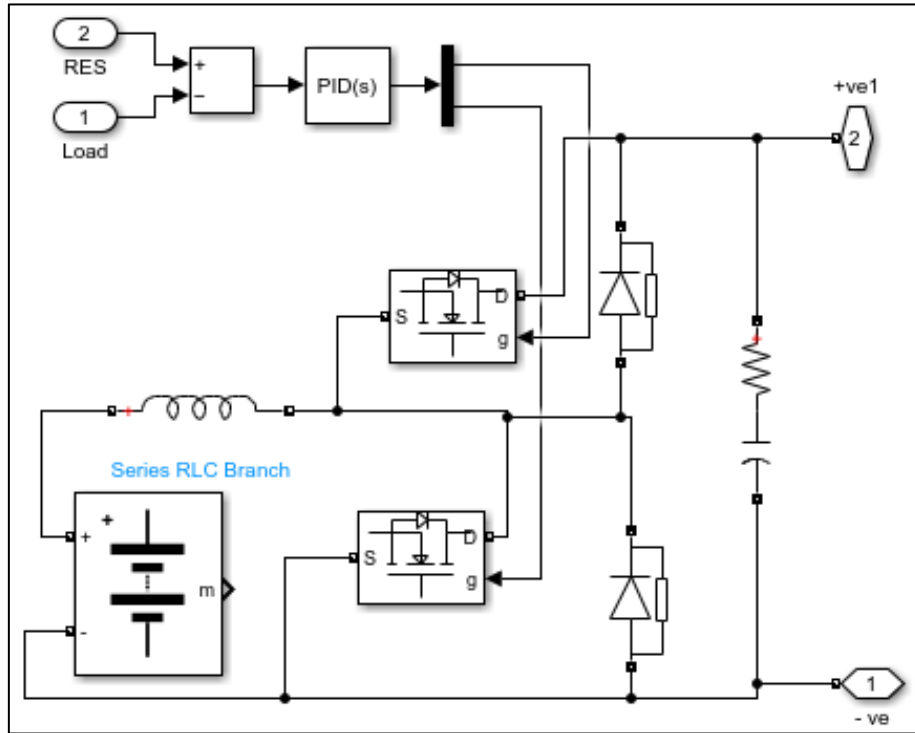


Figure 10. Bidirectional converter for battery storage system

4. SIMULATION RESULTS

It has been employed using MATLAB/Simulink to verify the proposed algorithm's performance. A 10kW grid connected with solar PV. The PV system consists of 5 modeled parallel and 10 PV strings in series. The solar PV specifications are illustrated in Fig. 5. A DC-DC boost converter relates to solar PV to energize the three-phase inverter. Two inverter control loops have been used for current and voltage control loops. The PO-MPPT and INC-MPPT achieve the MP drain from the PV system during the partial shading. The irradiance variation is shown in Fig. 11. The PV power, DC PV voltage, and the PV current responses for static and dynamic load are shown in Figs. 12 and 13, respectively. There is an oscillation in the obtained responses. Figs. 14 and 15 show the PV power, voltage, and current for the INC-MPPT method for static and dynamic loads, respectively. It can be observed that significant oscillation appeared in the responses.

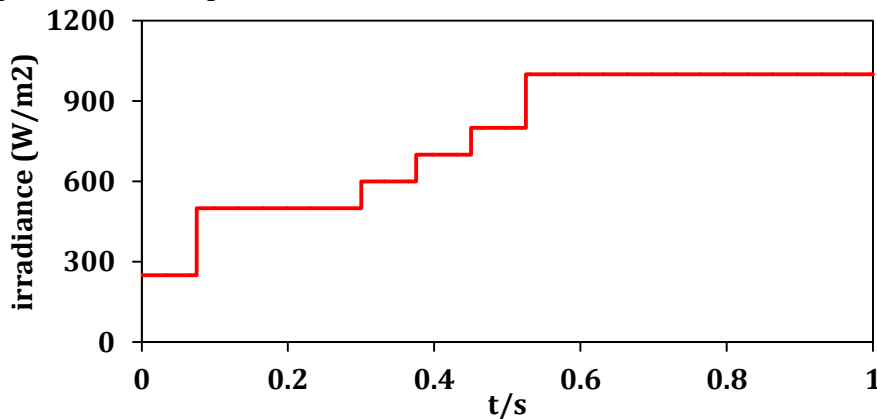


Figure 11. Irradiance variation

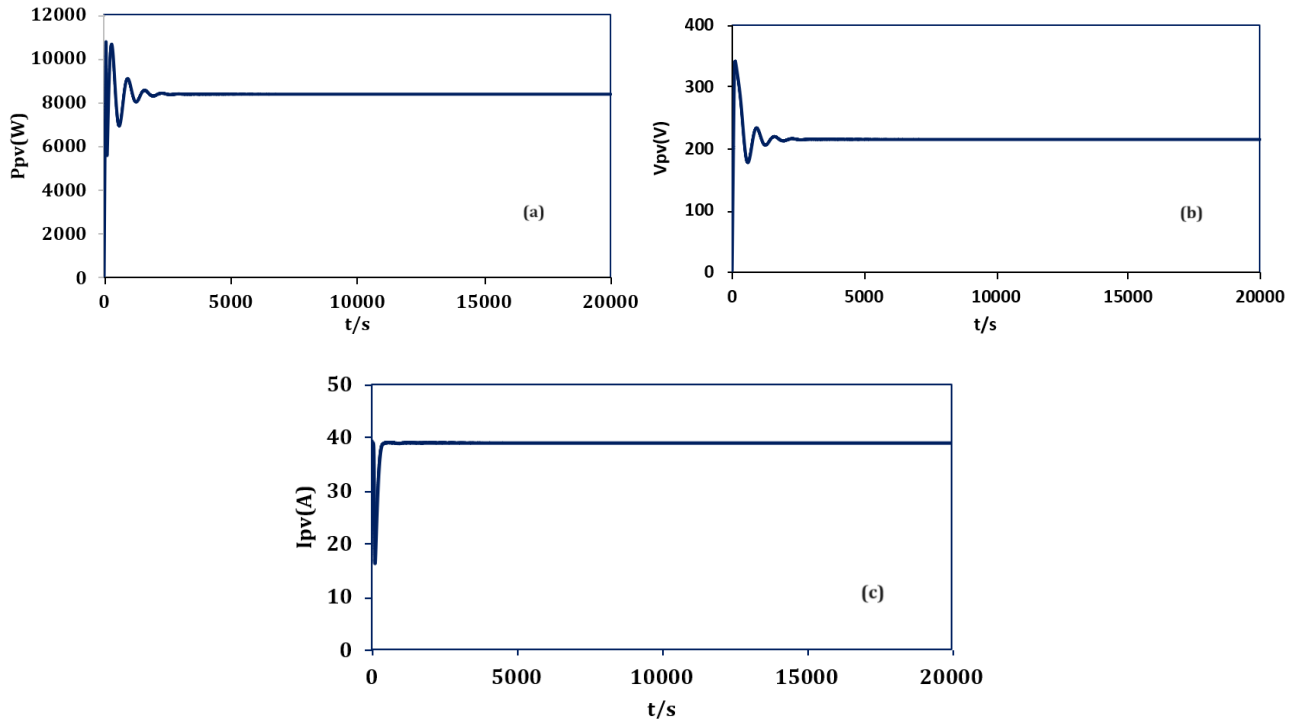


Figure 12. PO-MPPT for the static load (a) P_{pv} , (b) V_{pv} , and (c) I_{pv}

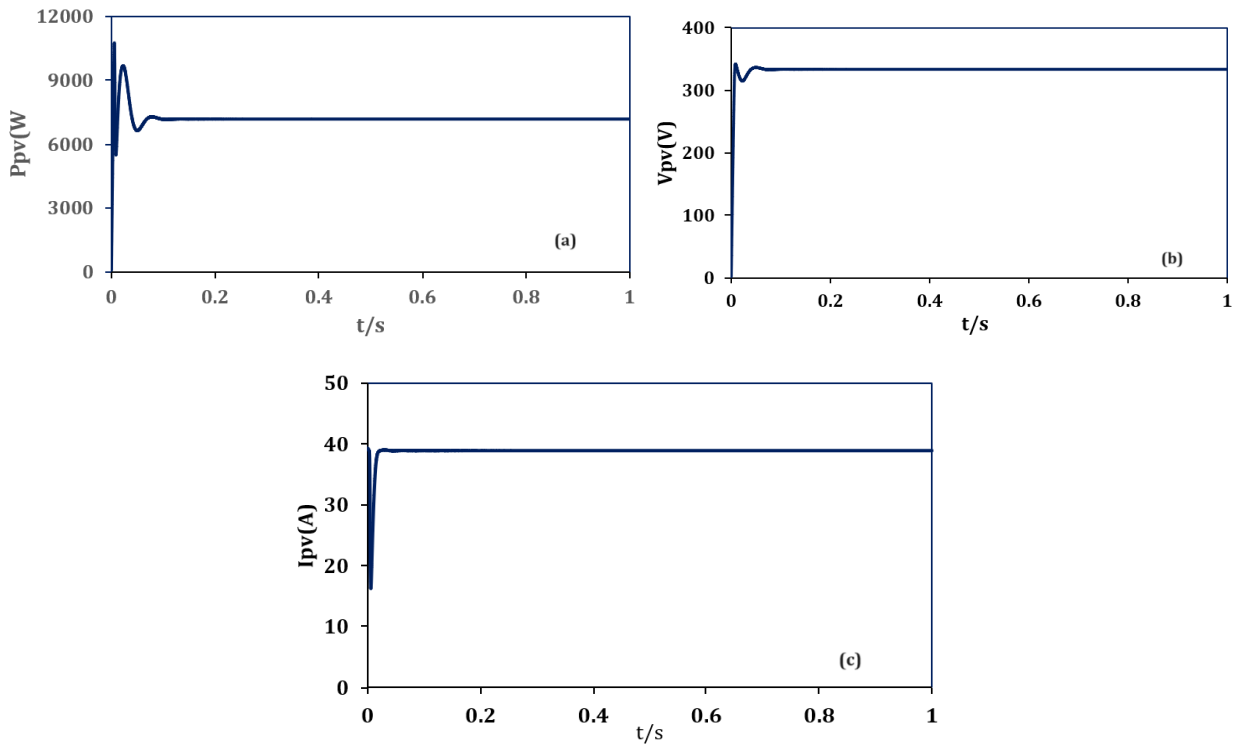


Figure 13. PO-MPPT for the dynamic load (a) P_{pv} , (b) V_{pv} , and (c) I_{pv}

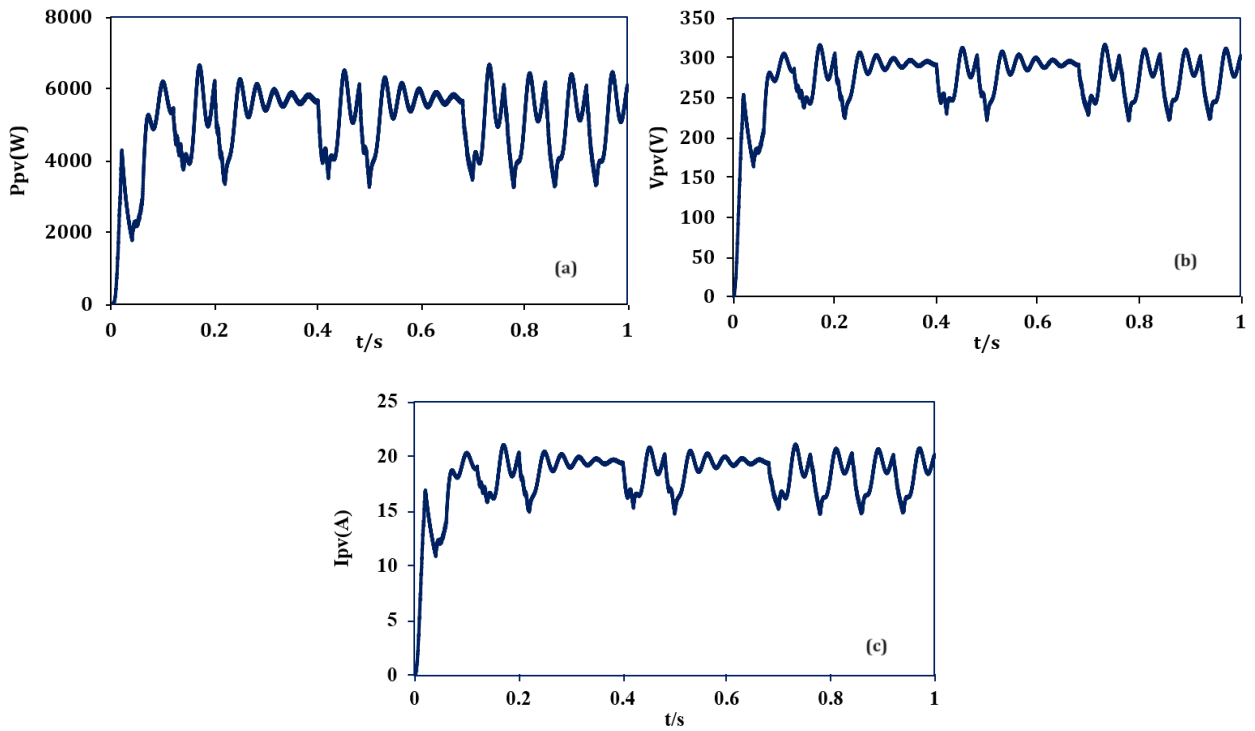


Figure 14. INC-MPPT for the static load (a) Ppv, (b)Vpv, and (c) Ipv

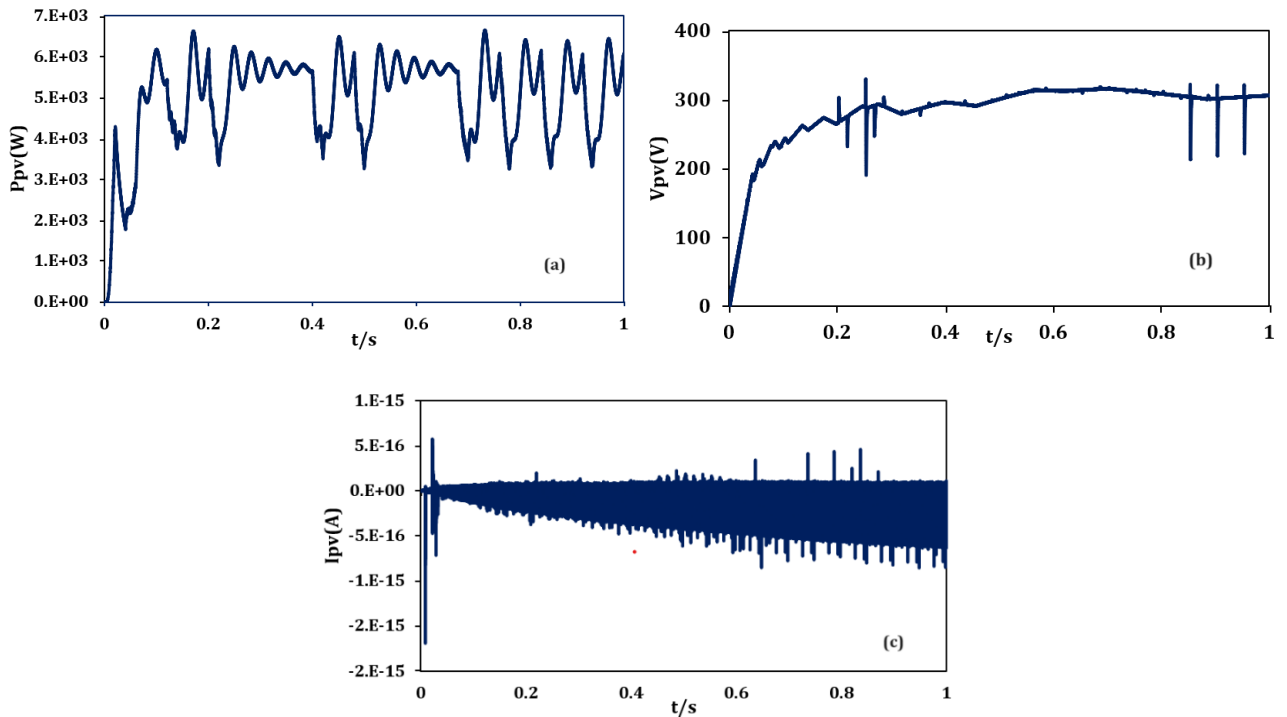


Figure 15. INC-MPPT for the dynamic load (a) Ppv, (b)Vpv, and (c) Ipv

Due to the drawbacks of the oscillation for the two MPPT methods (PO and INC), the NARMA-L2 has been used. The NARMA-L2 MPPT is utilized to control the boost converter to extract the MP by obtaining the desired output voltage of solar PV. The parameters of the proposed controller are shown in **Fig. 9**.

The simulation model has been approved for constant and variable irradiance profiles. The output power with and without the NARMA-L2 controller is shown in **Figs. 16** and **17** with constant irradiance ($1000\text{W}/\text{m}^2$) and variable irradiance profile respectively. **Table 2** tabulates the comparison of the performance of the MPPT strategies used in this paper.

The system is tested without NARMA-L2 MPPT and with NARMA-L2 for static load. The simulation results of the PV output power without and with NARMA-L2 MPPT output power for constant irradiance profile are shown in **Fig. 16**. It can be observed that the MPPT for NARMA-L2 controller had low steady-state error (low oscillation).

The simulation results of the PV output power without the NARMA-L2 controller and with NARMA-L2 MPPT output power with variable irradiance profile are shown in **Fig. 17**. It can be observed that the NARAM-L2 reaches MPPT with low oscillation and is softly adaptable to the irradiance variations. However, it is slower to reach the MPP than the conventional MPPT.

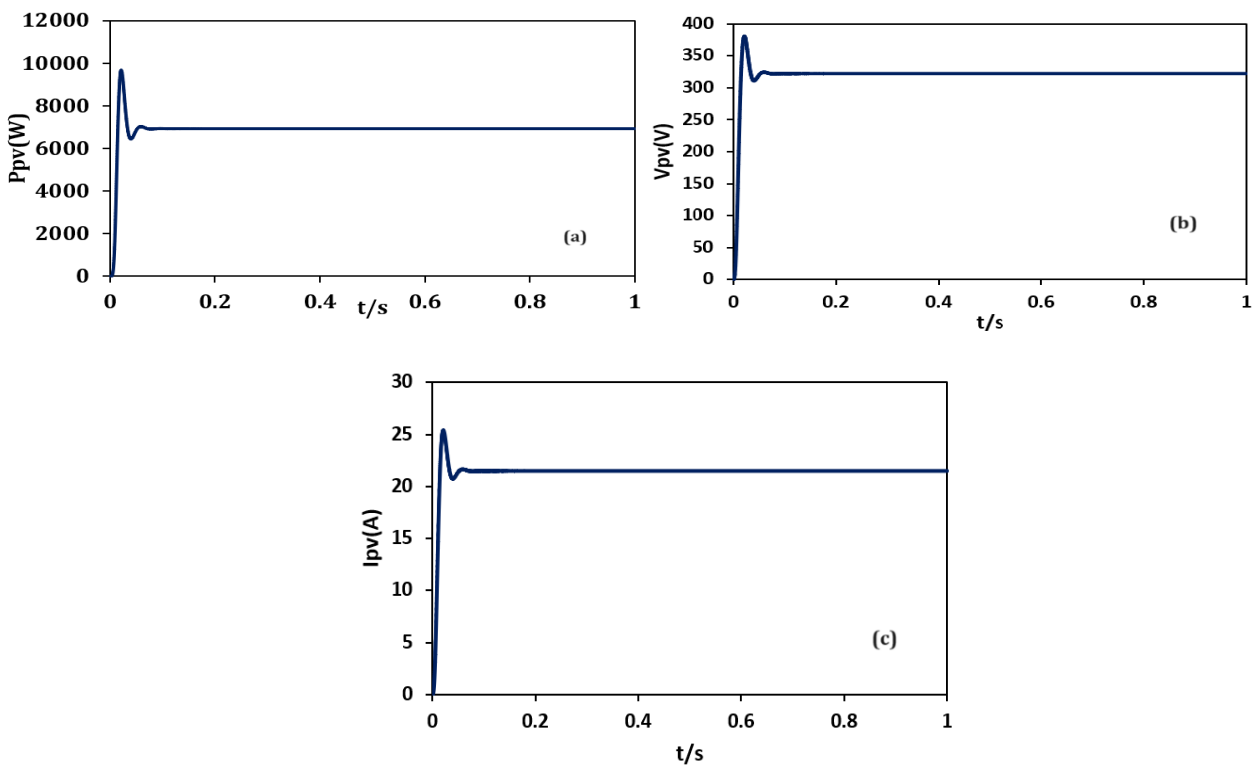


Figure 16. NARMA-L2 MPPT output for the static load (a) P_{pv} , (b) V_{pv} , and (c) I_{pv}

The system is tested under different types of loads (static and dynamic loads) to verify the proposed system's effectiveness and performance. **Fig. 18** shows the performance of the load voltage and current with the static load. **Fig. 19** shows the load voltage and load current under dynamic load. It is observed that the proposed system behavior does not influence the load type. The proposed MPPT algorithm optimizes the generation and demand powers.

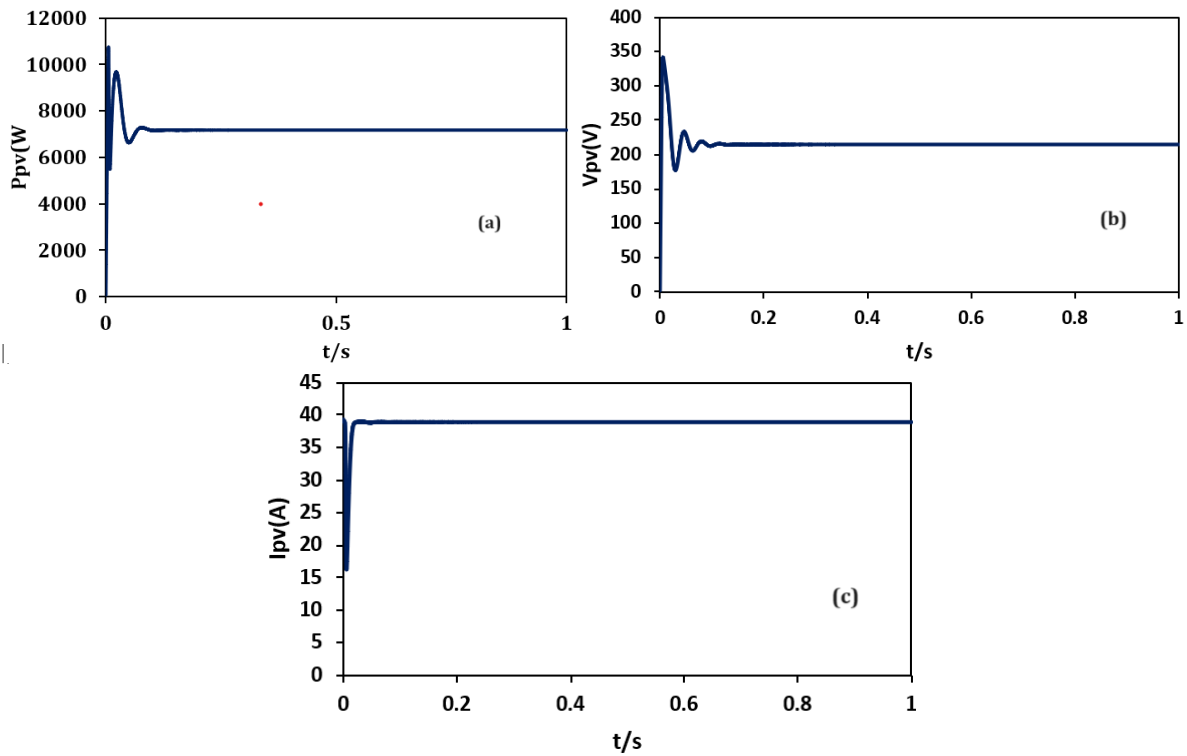


Figure 17. NARMA-L2 MPPT output for the dynamic load (a) Ppv, (b)Vpv, and (c)Ipv

Table 2. MPPT Strategies Comparison

MPPT strategy	Performance
P&O	Slow tracking speed, oscillations around MPPT, used with uniform solar array configuration and may struggle to handle complexity, slow convergence.
INC	Complex computations, unstable under partial shading
NARMA-L2	It is adaptive to track MPP, handling complex and nonlinearities, robust to weather variations and shading profiles, resilient to load dynamics, and fast response.

However, an optimal balance between the generated power from the PV solar and the demand power impacts the overall system efficiency and energy utilization. However, the dynamic load adds challenges to energy utilization. The simulation results illustrated the fast response, and the NARAM-L2 had more agile adjustments to track the varying MPP and verify the dynamic load requirements. It can figure out the implementation of deep learning NARAM-L2 controller MPPT for different loads, as given in **Table 3**.

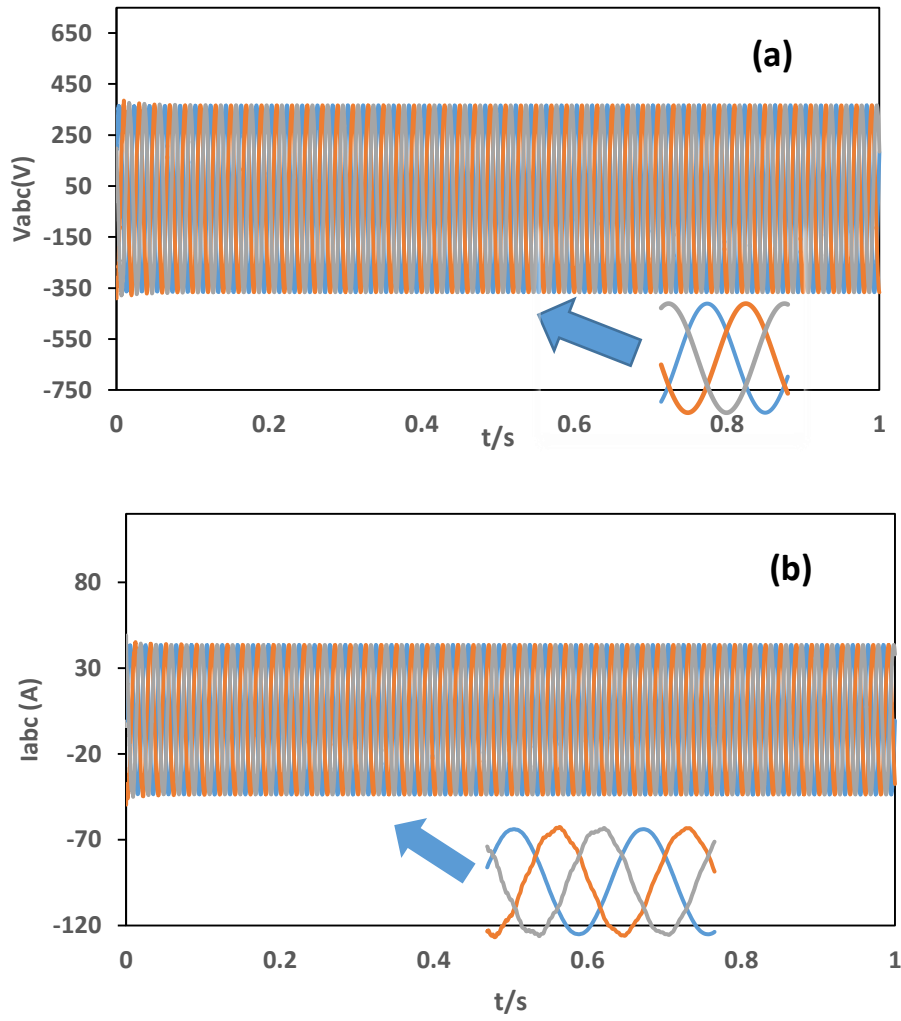
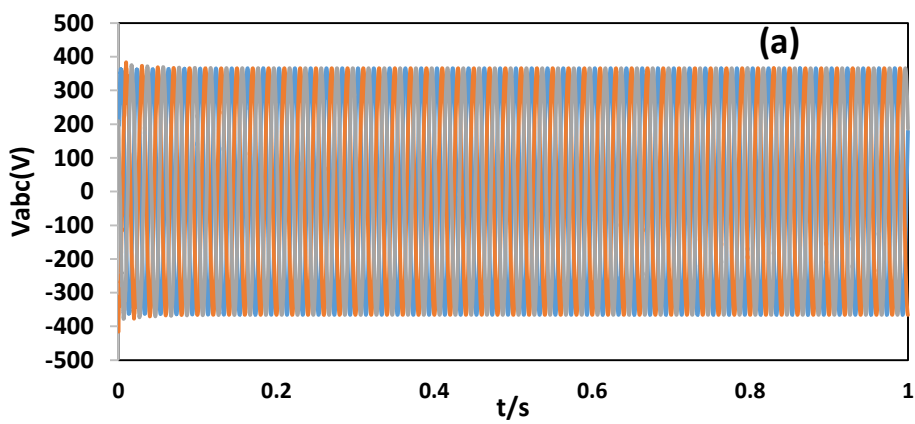


Figure 18. (a) load voltage and (b) current responses (with static load)



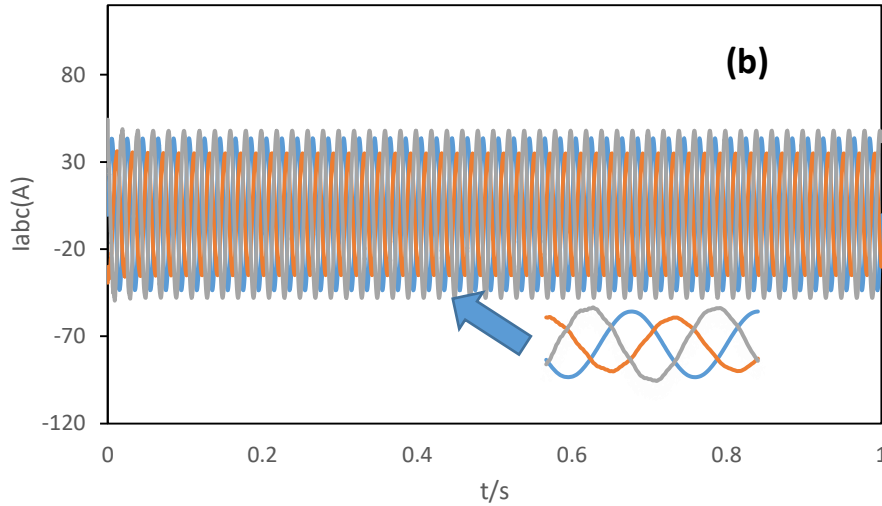


Figure 19. (a) load voltage and (b) current responses (with dynamic load)

Table 3. MPPT based on NARMA-L2 controller with different loads Comparison.

Type of load	Performance
static	constant power consumption, stable and efficient in partial shading conditions
dynamic	Unpredictable power changes, Deep learning MPPT adapts the power extraction, system efficiency, and energy utilization.

5. CONCLUSIONS

This paper presents MPPT algorithms under partial shading. Although the conventional MPPT methods, such as PO-MPPT and INC-MPPT. These methods are simple and easy to implement, but they have limitations in addressing challenging conditions such as irradiance variations and dynamic load. Therefore, a deep learning toolbox NARMA-L2 controller is proposed and used to track PV solar MPP. This controller can effectively handle the dynamic behavior of PV solar in real-time. As well as it has an advantage in adapting the changing irradiance to enhance the system performance and is capable of harvesting the energy while balancing the generated and consumed powers. Moreover, the NARMA-L2 controller is tested for dynamic load. The simulation results demonstrate the effectiveness of the NARMA-L2 in tracking the global MPP under different irradiance profiles, and it achieves a good response of load voltage and current for static and dynamic loads.



List of symbols

Symbol	definition	Symbo l	definition
I_o	reverse saturation current of the diode	Ppv	output PV power (W)
I_{ph}	photocurrent created by the cell	Iabc	load current (A)
K	Boltzmann’s constant (1.3805×10^{-23} J/K).	Vabc	load voltage (V)
n	ideality factor of the diode	Abbreviations	
q	charge of the electron ($1.6 \times 10^{-19}C$)	HER	Hybrid energy renewable
R_s	series resistance in PV cell	MPPT	Maximum power point tracking
R_{sh}	shunt resistance in PV cell	SOC	State of charge
T	temperature of the cell	PO	Perturb and observe
V_T	thermal tension of PV cell	INC	Increment conductance
V_{pv}	PV voltage (V)	PV	Photovoltaic
I_{pv}	PV current (A)		

REFERENCES

Abdul Hussain, A.M., and Habbi, H.M.D., 2018. Maximum power point tracking photovoltaic fed pumping system based on PI controller, in 2018 Third Scientific Conference of Electrical Engineering (SCEE). *IEEE Access*, pp. 78–83. [Doi:10.1109/SCEE.2018.8684120](https://doi.org/10.1109/SCEE.2018.8684120)

Ahmed, M., Harbi, I., Kennel, R., Rodriguez, J., and Abdelrahem, M., 2022. Model-based maximum power point tracking algorithm with constant power generation capability and fast DC-Link dynamics for two-stage PV systems. *IEEE Access*, 10, pp. 48551–48568. [Doi:10.1109/ACCESS.2022.3172292](https://doi.org/10.1109/ACCESS.2022.3172292)

Alcaide, A.M., Gomez-Merchan, R., Zafra, E., Martin, E.P., Rodriguez, J.Ml., Leon, J.I., Vazquez, S., and Franquelo, L.G., 2022. The Influence of MPPT Algorithms in the Lifespan of the Capacitor Across the PV Array. *IEEE Access* 10, pp. 40945–40952. [Doi:10.1109/ACCESS.2022.3164411](https://doi.org/10.1109/ACCESS.2022.3164411)

Asadi, Y., Eskandari, M., Mansouri, M., Moradi, M.H., and Savkin, A.V., 2023. A universal model for power converters of battery energy storage systems utilizing the impedance-shaping concepts. *International Journal of Electrical Power & Energy Systems*, 149, P. 109055. [Doi:10.1016/j.ijepes.2023.109055](https://doi.org/10.1016/j.ijepes.2023.109055)

Awan, M.M.A., Javed, M.Y., Asghar, A.B., and Ejsmont, K., 2022. Performance optimization of a ten check MPPT algorithm for an off-grid solar photovoltaic system. *Energies*, 15(6), P. 2104. [Doi:10.3390/en15062104](https://doi.org/10.3390/en15062104)

Azeem, F., Ahmad, A., Gondal, T.M., Arshad, J., Rehman, A.U., Eldin, E.M.T., Shafiq, M., and Hamam, H., 2022. Load management and optimal sizing of special-purpose microgrids using two stage PSO-fuzzy based hybrid approach. *Energies*, 15(17), P. 6465. [Doi:10.3390/en15176465](https://doi.org/10.3390/en15176465)



- Burlacu, M., and Navrapescu, V., 2022. Performance analysis of metaheuristic algorithms for optimal reactive power control in microgrids, in EPE 2022 - Proceedings of the 2022 12th International Conference and Exposition on Electrical and Power Engineering. Institute of Electrical and Electronics Engineers Inc., pp. 511–515. [Doi:10.1109/EPE56121.2022.9959843](https://doi.org/10.1109/EPE56121.2022.9959843)
- Chauhan, S., and Singh, B., 2022. Control of Solar PV Arrays Based Microgrid Intertied to a 3-Phase 4-Wire Distribution Network. *IEEE Trans Ind Appl* 58, pp. 5365–5382. [Doi:10.1109/TIA.2022.3171529](https://doi.org/10.1109/TIA.2022.3171529)
- Chen, C., Wang, Y., Cui, M., Zhao, J., Bi, W., Chen, Y., and Zhang, X., 2022. Data-driven detection of stealthy false data injection attack against power system state estimation. *IEEE Trans Industr Inform*, 18, pp. 8467–8476. [Doi:10.1109/TII.2022.3149106](https://doi.org/10.1109/TII.2022.3149106)
- Dagal, I., Akin, B., and Akboy, E., 2022. MPPT mechanism based on novel hybrid particle swarm optimization and salp swarm optimization algorithm for battery charging through simulink. *Scientific reports*, 12(1), P.2664. [Doi:10.1038/s41598-022-06609-6](https://doi.org/10.1038/s41598-022-06609-6)
- Gadiraju, H.K.V., 2022. Improved performance of PV water pumping system using dynamic reconfiguration algorithm under partial shading conditions. *CPSS Transactions on Power Electronics and Applications*, 7, pp. 206–215. [Doi:10.24295/CPSSTPEA.2022.00019](https://doi.org/10.24295/CPSSTPEA.2022.00019)
- Habbi, H.M., and Alhamadani, A., 2018. Power system stabilizer PSS4B model for Iraqi national grid using PSS/E software. *Journal of Engineering* 24(3), pp. 29–45. [Doi:10.31026/j.eng.2018.05.03](https://doi.org/10.31026/j.eng.2018.05.03)
- He, P., Li, Z., Jin, H., Zhao, C., Fan, J., and Wu, X., 2023. An adaptive VSG control strategy of battery energy storage system for power system frequency stability enhancement. *International Journal of Electrical Power and Energy Systems*, 149, P. 109039. [Doi:10.1016/j.ijepes.2023.109039](https://doi.org/10.1016/j.ijepes.2023.109039)
- Isknan, I., Asbayou, A., Hamid Adaliou, A., Ihlal, A., and Bouhouch, L., 2023. Comparative study and simulation of advanced MPPT control algorithms for a photovoltaic system. *Indonesian Journal of Electrical Engineering and Computer Science*, 30(46), pp. 46-56. [Doi:10.11591/ijeecs.v30.i1](https://doi.org/10.11591/ijeecs.v30.i1)
- Jamil, H., Qayyum, F., Iqbal, N., and Kim, D.-H., 2022. Enhanced harmonics reactive power control strategy based on multilevel inverter using ML-FFNN for dynamic power load management in microgrid. *Sensors*, 22, P. 6402. [Doi:10.3390/s22176402](https://doi.org/10.3390/s22176402)
- Jane, R.S., Vaucher, G., Berman, M., and Parker, G., 2022. Military operations research society optimizing tactical microgrid operation using in-situ forecasting techniques. *Source: Military Operations Research*, 27, pp. 25–44. [Doi:10.2307/27140354](https://doi.org/10.2307/27140354)
- Kaushal, J., and Basak, P., 2020. Power quality control based on voltage sag/swell, unbalancing, frequency, THD and power factor using artificial neural network in PV integrated AC microgrid. *Sustainable Energy, Grids and Networks*, 23, P. 100365. [Doi:10.1016/j.segan.2020.100365](https://doi.org/10.1016/j.segan.2020.100365)
- Kulkarni, P., and Deshmukh, S.P., 2019. Different converter topologies for solar photovoltaic system with methods for maximum power point tracking algorithms. *International Journal of Innovative Technology and Exploring Engineering*, 8, pp. 1112–1118. [Doi:10.35940/ijitee.J1202.0981119](https://doi.org/10.35940/ijitee.J1202.0981119)
- Millah, I.S., Chang, P.C., Teshome, D.F., Subroto, R.K., Lian, K.L., and Lin, J.F., 2022. An enhanced grey wolf optimization algorithm for photovoltaic maximum power point tracking control under partial shading conditions. *IEEE Open Journal of the Industrial Electronics Society*, 3, pp. 392–408. [Doi:10.1109/OJIES.2022.3179284](https://doi.org/10.1109/OJIES.2022.3179284)
- Millah, I.S., Subroto, R.K., Chang, Y.W., Lian, K.L., and Ke, B.R., 2021. Investigation of maximum power point tracking of different kinds of solar panels under partial shading conditions. *IEEE Trans Ind, Appl* 57, pp. 17–25. [Doi:10.1109/TIA.2020.3029998](https://doi.org/10.1109/TIA.2020.3029998)



- Mohamed, H.A., and Habbi, H.M., 2020. Power quality of dual two-level inverter fed open end winding induction motor. *Indonesian Journal of Electrical Engineering and Computer Science*, 18, pp. 688-697. [Doi:10.11591/ijeecs.v18.i2.pp688-697](https://doi.org/10.11591/ijeecs.v18.i2.pp688-697)
- Paduani, V.D., Yu, H., Xu, B., and Lu, N., 2022. A Unified power-setpoint tracking algorithm for utility-scale pv systems with power reserves and fast frequency response capabilities. *IEEE Trans Sustain Energy*, 13, pp. 479–490. [Doi:10.1109/TSTE.2021.3117688](https://doi.org/10.1109/TSTE.2021.3117688)
- Pendem, S.R., and Mikkili, S., 2018. Modeling, simulation and performance analysis of solar PV array configurations (Series, Series-Parallel and Honey-Comb) to extract maximum power under Partial Shading Conditions. *Energy Reports*, 4, pp. 274–287. [Doi:10.1016/j.egyr.2018.03.003](https://doi.org/10.1016/j.egyr.2018.03.003)
- Pervez, I., Antoniadis, C., and Massoud, Y., 2022. A reduced search space exploration metaheuristic algorithm for MPPT. *IEEE Access*, 10, pp. 26090–26100. [Doi:10.1109/ACCESS.2022.3156124](https://doi.org/10.1109/ACCESS.2022.3156124)
- Rao, V.S., and Sundaramoorthy, K., 2022. Performance analysis of voltage multiplier coupled cascaded boost converter with solar PV integration for DC microgrid application. *IEEE Transactions on Industry Applications*, 59(1), pp.1013-1023. [Doi:10.1109/TIA.2022.3209616](https://doi.org/10.1109/TIA.2022.3209616)
- Saadaoui, K., Rhazi, K.S., Mejdoub, Y., and Aboudou, A., 2023. Modelling and simulation for energy management of a hybrid microgrid with droop controller. *International Journal of Electrical and Computer Engineering (IJECE)*, 13, P. 2440. [Doi:10.11591/ijece.v13i3.pp2440-2448](https://doi.org/10.11591/ijece.v13i3.pp2440-2448)
- Singh, M., V, M.H., S, V.H., 2022. Investigation on power system stability with integration of renewable resources. 2022 IEEE 10th Power India International Conference (PIICON). IEEE, pp. 1–6. [Doi:10.1109/PIICON56320.2022.10045098](https://doi.org/10.1109/PIICON56320.2022.10045098)
- Nhung, L.T.H., Phung, T.T., Nguyen, H.M.V., Le, T.N., Nguyen, T.A., and Vo, T.D., 2022. Load shedding in microgrids with dual neural networks and AHP algorithm. *Engineering, Technology & Applied Science Research*, 12(1), pp. 8090-8095. [Doi:10.48084/etasr.4652](https://doi.org/10.48084/etasr.4652)
- Vanti, S., Bana, P.R., D'Arco, S., and Amin, M., 2022. Single-stage grid-connected PV system with finite control set model predictive control and an improved maximum power point tracking. *IEEE Trans Sustain Energy*, 13, pp. 791–802. [Doi:10.1109/TSTE.2021.3132057](https://doi.org/10.1109/TSTE.2021.3132057)
- Wen, L., Zhou, K., Yang, S., and Lu, X., 2019. Optimal load dispatch of community microgrid with deep learning based solar power and load forecasting. *Energy*, 171, pp. 1053–1065. [Doi:10.1016/j.energy.2019.01.075](https://doi.org/10.1016/j.energy.2019.01.075)
- Yang, M., Cui, Y., and Wang, J., 2023. Multi-Objective optimal scheduling of island microgrids considering the uncertainty of renewable energy output. *International Journal of Electrical Power & Energy Systems*, 144, P. 108619. [Doi:10.1016/j.ijepes.2022.108619](https://doi.org/10.1016/j.ijepes.2022.108619)
- Zhou, L., Chen, Y., Luo, A., Guerrero, J.M., Zhou, X., Chen, Z., and Wu, W., 2016. Robust two degrees-of-freedom single-current control strategy for LCL-type grid-connected DG system under grid-frequency fluctuation and grid-impedance variation. *IET Power Electronics*, 9, pp. 2682–2691. [Doi:10.1049/iet-pel.2016.0120](https://doi.org/10.1049/iet-pel.2016.0120)



Appendix A

PO-MPPT and INC-MPPT algorithms

```

di=i-io;
d=0.00055;
if du==0
    if di==0
        s=D;
    else
        if di>0
            s=D-d;
        else
            s=D+d;
        end
    end
else
    if di/du== -(i/u)
        s=D;
    else
        if di/du> -(i/u)
            s=D-d;
        else
            s=D+d;
        end
    end
end
f = s;
end

```

```

S.P=P;
end
function D = MPPT
(V,v,P,p,d)
d=0.58;
dv=V-v;
dp=P-p;
if(dp>0)
    if(dv<0)
        D=d+0.05;
    else
        D=d-0.05;
    end
else
    if(dv<0)
        D=d-0.05;
    else
        D=d+0.05;
    end
end
end
Matlab function for INC-
MPPT algorithm
function y =
MYMPP(u,i,uo,io,D)
s=0.4;
du=u-u0;

```

```

Matlab function for PO-
MPPT
function D =
fcn(V,I,dD,Dini)
%% Memory Storage
persistent S
if isempty(S)
    S.D=Dini; % Initial
Duty Cycle
    S.V=0;
    S.P=0;
end

%% Pn0 Algorithm
P=V*I;
dV=V-S.V;
dP=P-S.P;
dPV=dV*dP;
if dPV>0
    D=S.D-dD;
else
    D=S.D+dD;
end

%% Update Memory
S.D=D; % Initial Duty
Cycle
S.V=V;

```